

Filamentation due to the Weibel Instability in two counter-streaming laser ablated plasmas

Quan-Li Dong^{1,*}, Dawei Yuan^{2,3}, Lan Gao⁴, Xun Liu², Yangao Chen⁴, Qing Jia⁴, Neng Hua⁵, Zhanfeng Qiao⁵, Ming Chen⁵, Baoqiang Zhu⁵, Jianqiang Zhu⁵, Gang Zhao³, Hantao Ji⁴, Zheng-Ming Sheng⁶, Jie Zhang⁶

1 School of physics and optoengineerings, Ludong University, Yantai 264025, China;

2 Institute of Physics, CAS, Beijing 100190, China;

3 National Astronomical Observatories, CAS, Beijing 100012, China;

4 PPPL, Princeton University, Princeton, New Jersey 08543, USA;

5 National Laboratory on High Power Lasers and Physics, Shanghai, 201800, China;

6 Key Laboratory for Laser Plasmas (MoE) and Department of Physics, Shanghai Jiao Tong University, Shanghai 200240, China

* qldong@aphy.iphy.ac.cn

Abstract. Weibel-type filamentation instability was observed in the interaction of two counter streaming laser ablated plasma flows, which were supersonic, collisionless, and closely relevant to astrophysical conditions. The plasma flows were created by irradiating a pair of oppositely standing plastic (CH) foils with 1ns-pulsed laser beams of total energy of 1.7 kJ in two laser spots. With characteristics diagnosed in experiments, the calculated features of Weibel-type filaments are in good agreement with measurements.

1. Introduction

The physical mechanisms of magnetic field generation, amplification and annihilation play important roles in many astrophysical phenomena. Take the SN1006 as example. One explanation for surrounding shock structures is that the magnetic field are generated through Weibel Instability (WI) during interaction between outflow plasmas, reorganized and amplified, forming transverse structure (perpendicular to plasma flow direction) at large scales and capturing/stagnating incident charged particles to form shocks within which they accelerate and irradiate the synchrotron emission, manifesting magnetic field configuration they are gyrating around [1,2]. Following the above hyperthesis for shocks and ultrahigh energy cosmic rays from supernova, laboratory laser-plasma experiments designed for astrophysics study have to demonstrate, step by step, the magnetic field generation and amplification, charged particle acceleration and gyration to radiate synchrotron emission [3-6].

This paper reports density observations of Weibel-type filamentation of counter streaming laser plasmas, which act as the supplement for the magnetic filaments observed in [7]. However the filamentation instability is still far from nonlinear regime, indicating large laser facility is needed for WI mediated collisionless shock study.

2. Experiment setup



Experiments were conducted on the SG-II laser facility platform in September, 2011. The setup is shown in Figure 1. Two face-to-face standing CH foil targets of $5 \times 5 \text{ mm}^2$ were used to generate a pair of counterstreaming plasma flows. To produce asymmetrical plasma flows, seven 1ns-pulsed laser beams were launched and divided into two groups: the 4 southern laser beams of 1 kJ were focused on the northern target, and the 3 northern of 0.7 kJ on the southern target. The southern bunch of laser beams was delayed by 1ns making sure that two plasma flows have different properties when they encounter between two CH foils separated by 4.5 mm. The laser spots on CH foils were 150 μm in diameter, generating an average laser intensity of 10^{14} – 10^{15} W/cm^2 . The 9th laser beam of SG-II platform was used as a probe to measure the plasma density profile through Normaski Interferometry (NI) and shadowgraphy techniques. With the probe of 2ω (527 nm in wavelength) and 30 ps duration was applied, the upper measurement limit of the electron density is around $5\text{--}8 \times 10^{19} \text{ cm}^{-3}$ in our experiments. At different delay times with respect to the southern bunch, the recorded interferometry can provide the temporal evolution of the electron density. One interferometry image and one shadowgraphy image are given as examples, which are also the main objectives for our analysis. For all shots, x-ray pinhole cameras of 10 time magnification were also used to measure the uniformity of the laser spots.

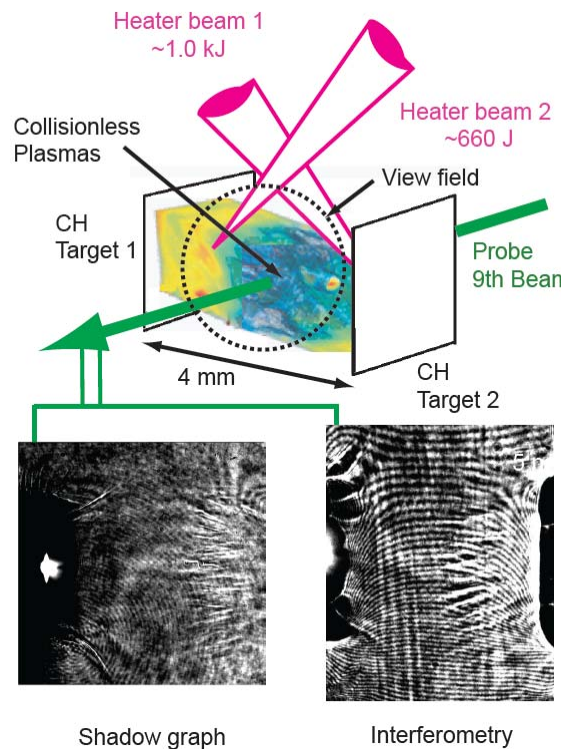


Figure 1. Experimental setup. Two oppositely standing CH foil targets were irradiated by 1ns-pulsed laser bunches with energy 1.0 kJ and 0.7 kJ, respectively. The 9th beam of SG II was used to probe the colliding plasmas, producing interferometry and shadowgraphy images of which two examples were given for 4.5 ns delay measurements.

3. Experimental result analysis

Figure 2 shows the recorded shadowgraphy at time delay of 4.5 ns. The main feature is the filaments that follow the expansion direction of the right plasma ball. The filament location near the side of the right (northern) laser spot rather than the center is attributed to 1-ns-delay of launch time of the Southern bunch lasers. The shot time arrangement of as well as the different energy contained in two laser spots produced a condition with tenuous background plasma for the hotter plasma from the right target, while avoiding the Southern laser heating of the preformed plasma. The indicated over dense plasma region shows the edge of plasma with density higher than $5 \times 10^{19} \text{ cm}^{-3}$. The filaments can be divided into two groups according to their lengths. The longer filaments are supposed to be located in or parallel to face-on planes containing two laser spots, while shorter filaments are supposed to be the

projections of those filaments with larger angles to face-on planes. The dashed line gives the position where the filament distribution pattern is analyzed in Figure 3.

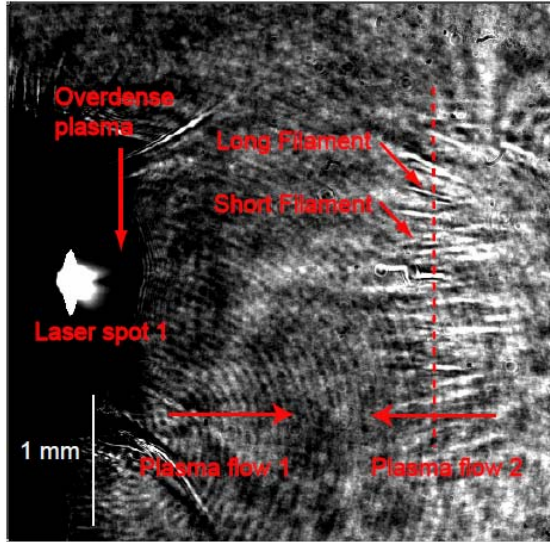


Figure 2. Shadowgraphy taken at 4.5 ns delay with respect to the tail of the laser pulse. The width distribution of the spaces between filaments along the dashed line will be analyzed in Figure 3.

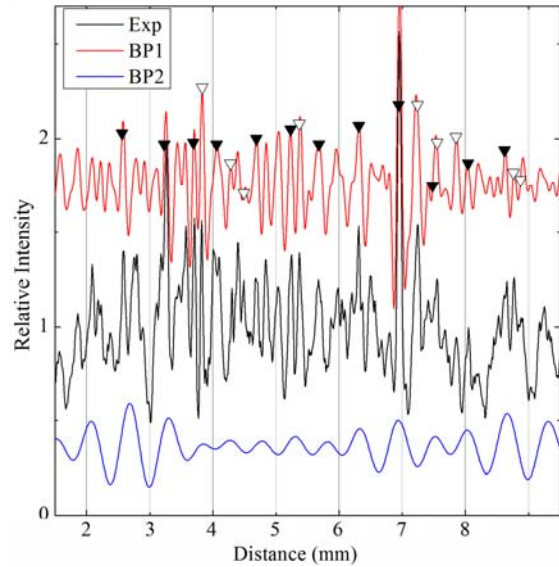


Figure 3. Profile of the filament distribution along the dashed line in Figure 1. The black line is the experimental result. With different band FFT (Fast Fourier Transformation) filters, the red line presents all (short and long) filaments spaced by 90-250 μm , while the blue line presents only long filaments spaced by 400-600 μm as indicated by the solid triangles.

The profile of the filament distribution is analyzed by using different band FFT (Fast Fourier Transformation) filters. The red line presents the filtered profile involving all (short and long) filaments spaced by 90-250 μm , while the blue line presents only long filaments spaced by 400-600 μm as indicated by the solid triangles. Both FFT-filtered distributions reproduce the corresponding peaks /filaments in the experimental profile. It can be expected that the spaces between real filaments in 3D is 400-600 μm , and the smaller value of 90-250 μm is due to the "forest-effect" the projection process usually has.

To explore the mechanisms underlying the filamentation, growth rates were calculated for various instabilities with the diagnosed plasma parameters. It is found that for the filamentation parallel to the flow velocity, Weibel instability is the most likely mechanism. The dispersion relation of the beam-Weibel instability is given by:

$$\omega^2 = (kc)^2 - \sum_s \omega_{ps}^2 \left[\frac{v_{sth}^2 + 2(V_s \sin(\theta))^2}{v_{sth}} (1 + \zeta_s Z(\zeta_s)) - 1 \right]$$

where $Z(\zeta) \equiv \pi^{-1/2} \int_{-\infty}^{\infty} \frac{e^{-z^2}}{z - \zeta} dz$ is the dispersion function, $\zeta_s = \zeta_s(\omega, k, \theta) \equiv (\omega/k - V_s \cos(\theta))/v_{sth}$,

with V_s the bulk velocity, and $v_{sth} = \sqrt{2T/m}$ is the average thermal velocity at temperature T . The calculation result is shown in Figure 4, indicating the Weibel instability grew at $\gamma \sim 4 \times 10^{-5} \omega_{pe}$ and $k c / \omega_{pe} \sim 0.17$, which means, for plasmas with electron density of $5 \times 10^{18} \text{ cm}^{-3}$ that can be measured by the interferometry technique, the space between filaments is around 480 μm , agreeing well with the measurements. With the calculated growth rate, the amplitude of filamentations will grow by hundreds

of times in several nanoseconds, making it observable but still in weak linear regime as indicated by the ratios ($\gg 1$) of the filament length (or the parallel wavelength) and the space (or the perpendicular wavelength) to the diameter of filaments.

Contributions to growth rates from different plasma properties were also studied. As CH plasma contains various carbon ions, to simplify the calculation C^{4+} and H^+ were adopted. Growth rates of following cases were calculated: plasma-plasma interactions, plasma-ion-beam interaction, and plasma-electron-beam interaction. The growth rates changed little for three different cases with the same bulk velocity. But for higher bulk velocity, the growth rate increased significantly.

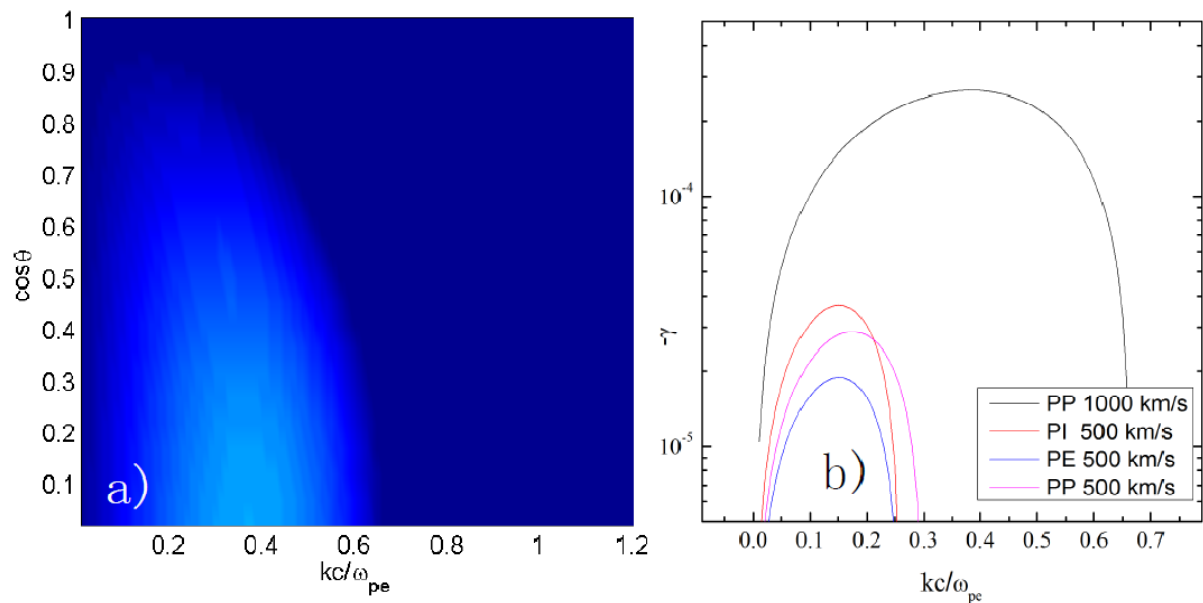


Figure 4. **a)** Growth rate of Weibel-type filamentation instability in the pair of counterstreaming laser plasmas with experimental conditions. **b)** Growth rate γ of filamentations parallel to plasma bulk velocity v_b . Effects of different components to γ were compared. PP 1000km/s represents for plasma-plasma interaction with $v_b = 1000\text{km/s}$; PI for plasma-ion-beam interaction, and PE for plasma-electron-beam interaction.

4. Summary

A pair of counterstreaming laser plasmas were found to have filamentation behavior which were attributed to Weibel instability. However, the instability is still in linear regime, and the magnetic field is weak, far from the strength needed for stagnating charged particles to form collisionless shocks as observed in SN remnants. Larger plasma systems allowing for longer interaction time might help Weibel instability evolve into nonlinear regime necessary for laboratory study of collisionless shock related ultra high energy cosmic rays.

This work is jointly supported by the National Natural Science Foundation of China (Grants No. 11274152 and No. 11220101002).

References

- [1] G. Cassam-Chenai et al., *Astrophys. J.* **680**, 1180 (2008);
- [2] Francisco Suzuki-Vidal et al., *Nature Physics* **11**, 98 (2015);
- [3] Hideaki Takabe et al., *Plasma Phys. Control. Fusion* **50**, 124057 (2008);
- [4] R. P. Drake and G. Gregori, *Astrophys. J.* **749**, 171 (2012);
- [5] Will Fox et al., *Phys. Rev. Lett.* **111**, 225002 (2013);
- [6] K. Quinn et al., *Phys. Rev. Lett.* **108**, 135001 (2012);
- [7] C. M. Huntington et al., *Nature Physics* **11**, 173 (2015);